EurJIC
European Journal of Inorganic Chemistry

Research Article
doi.org/10.1002/ejic.202100988

Chemistry Europe
European Chemical Societies Publishing

www.eurjic.org

Special Collection

Enantioselective Pd-Catalyzed Allylic Substitution using Phosphite-Oxazoline PHOX-Based Ligands containing a Methylene Linker

Pol de la Cruz-Sánchez,[a] Maria Biosca,[a] Marc Magre,[a] Jorge Faiges,[a] Jéssica Margalef,*[a] Oscar Pàmies,[a] and Montserrat Diéguez*[a]

Dedicated to Professor Rinaldo Poli in occasion of his 65th birthday.

High enantioselectivities (up to 99%) and activities (TOF's up to $>4000\ h^{-1}$) are accomplished in the Pd-catalyzed allylic substitution of a wide range of substrate types and nucleophiles using a family of phosphite-oxazoline ligands. These ligands were derived from the PHOX ligand by exchanging the phosphine moieties by biaryl phosphites and a methylene spacer was introduced between the oxazoline and the phenyl ring. The wide substrate scope is due to the ability of the ligand family to adapt their ligand parameters to the reacting substrate. This ability also explains its high performance in other type of catalytic processes.

Introduction

Due to its mild reaction conditions, high functional group tolerance and the versatility of the alkene group for further functionalization, Pd-catalyzed asymmetric allylic substitution (AAS) is an efficient tool for the formation of chiral C–C and C-heteroatom bonds with applications in the synthesis of enantiomerically pure relevant compounds.[1] To fully exploit their application in total synthesis there is a constant need to expand the range of substrate and nucleophiles. Over the last decades a great number of ligands have been successfully applied for this transformation.[1] However, catalysts are hardly suitable for a wide combination of substrates and nucleophiles. In addition, most catalysts still have a pronounced substrate specificity, with sterically hindered substrates requiring different ligands than unhindered substrates.[1] To reduce time-consuming ligand design synthesis, catalysts with wide substrate and nucleophile scope are desired. The first breakthrough in ligand design was introduced by Trost with the development of diphosphine ligands, such as (*R*,*R*)-Ph-DACH **1**, with a large bite angle which creates a more confined chiral cavity (Figure 1).[2] The stereoselectivity comes from an interplay between steric interactions imposed by the chiral cavity of the ligand and the H-bond and the electrostatic interactions of the amide groups with the nucleophile.[3] Trost ligands represent one of the most effective ligand families and are the ligands of choice for unhindered substrates, being the most widespread applied in total synthesis.[1,4] Another relevant breakthrough arrived with the application of the heterodonor phosphine-oxazoline PHOX ligands **2** (Figure 1), whose application complemented the Trost ligands, providing high enantioselectivities with hindered substrates and low with narrow ones.[5] The stereoselectivity is based on the *trans* influence of the two donor groups that favors the nucleophilic attack predominantly trans to the donor group with the strongest trans influence. These facts, together with the excellent performance of PHOX ligands in other asymmetric unrelated catalytic reactions, have made them belong to the selected list of "privileged ligands".[6]

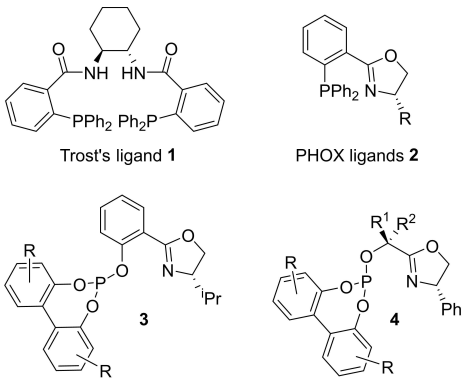

Figure 1. (*R*,*R*)-Ph-DACH Trost's ligand **1**, phosphine-oxazoline PHOX ligands **2**, phosphite-oxazoline based PHOX ligands **3** and phosphite-oxazoline ligands **4**.

Inspired by the PHOX ligands, heterodonor bidentated P,N- and P,X-ligands (X=P′ and S) have found a prominent position in the field of Pd-AAS, with the development of many new

[a] *P. de la Cruz-Sánchez, Dr. M. Biosca, Dr. M. Magre, J. Faiges, Dr. J. Margalef, Prof. O. Pàmies, Prof. M. Diéguez*
Departament de Química Física i Inorgànica,
Universitat Rovira i Virgili
C/ Marcel·lí Domingo, 1, 43007 Tarragona, Spain
E-mail: jessica.margalef@urv.cat
montserrat.dieguez@urv.cat

Supporting information for this article is available on the WWW under https://doi.org/10.1002/ejic.202100988

Part of the "celebratory collection for Rinaldo Poli".

Research Article
doi.org/10.1002/ejic.202100988

families that have provided remarkable results.[1,7,8] In this respect, our group has taken advantage of the adaptability of biaryl phosphite-based ligands to overcome the substrate specificity and low nucleophile scope of the Pd-AAS.[9] We found that the common substrate limitation of the phosphine-oxazoline PHOX-ligands **2** could be overcome by replacing the phosphine moiety by a biaryl phosphite group.[10] By introducing this group, the catalyst can adapt to each substrate and the substrate scope has been significantly broadened. Therefore, and in contrast to the parent PHOX ligands **2**, phosphite-oxazoline ligands **3** (Figure 1) show a wide substrate scope, providing high enantioselectivities for hindered and unhindered substrates, with a large variety of C, N and O-nucleophiles.[10] In addition, the acceptor capacity of the phosphite functionality had a positive effect on activity, inducing much higher TOF than the most common ligands. Since then, our group has developed other biaryl phosphite containing ligands, by modifying either the ligand backbone or by replacing the oxazoline by other N-donor groups[8i,k–n] (i.e. oxazole, pyridine, etc) and S-groups[,8j,11] with remarkable results. Among them, we can highlight the phosphite-oxazoline ligands **4**,[8p] where the *ortho*-phenylene tether of PHOX and of ligands **3** has been replaced by an alkyl backbone chain. Their Pd-catalysts provided enantioselectivities up to 99% in the allylic substitution of a wide range of substrate types and C, N and O-nucleophiles, even the challenging monosubstituted ones.

Combining the advantages of the biaryl phosphite groups and the backbone's structure of PHOX ligands, we have recently designed a set of phosphite-oxazoline ligands **L1**–**L3a**–**c** with a methylene spacer between the oxazoline ring and the phenyl ring (Figure 2), that were applied in two different asymmetric transformation (hydrogenation and intermolecular Heck reactions) extending the range of substrates and triflate sources successfully used.[12] In this report, we studied these ligands in the Pd-catalyzed allylic substitution reaction to further investigate the possibilities of easily to synthetize phosphite-analogues of PHOX-type ligands in Pd-AAS reactions. By tuning the ligand parameters, we have been able to achieve high enantioselectivities for a variety of substrates and nucleophiles (35 compounds in total). We have also performed DFT and NMR studies to gain further insight into the selectivity-determining step.

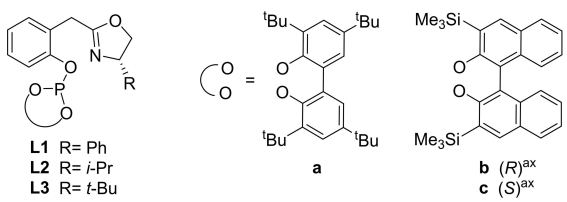

Figure 2. Phosphite-oxazoline ligands **L1**–**L3a**–**c** tested in this study.

Results and Discussion

Initial screening. Allylic substitution of two disubstituted substrates (S1 and S2) with different steric requirement using dimethyl malonate

The usefulness of ligands **L1**–**L3a**–**c** in Pd-AAS was first studied in the alkylation of two substrates with distinct steric properties, the benchmark lineal substrate *rac*-1,3-diphenyl-3-acetoxyprop-1-ene **S1** and the more challenging cyclic *rac*-3-acetoxycyclohexene **S2**. For comparison, we applied the same reaction conditions found in our previous studies with analogous Pd/**3** catalytic system, using dimethyl malonate as nucleophile (Table 1).[10b,13] Positively, high activities (TOF's up to >4000 mol substrate$\times$(mol Pd$\times$h)$^{-1}$) and enantioselectivities (ee's up to 96%) in both substrate types were obtained by selecting the right combination of oxazoline substituent and phosphite group. Concretely, the results showed that enantioselectivity depended on the biaryl phosphite group (**a**–**c**). For both substrates, ligands with an enantiopure (*S*)-biaryl phosphite functionality yielded the highest enantioselectivities (entries 3, 6 and 9 vs 1–2, 4–5 and 7–8, respectively). However, the effect of the oxazoline substituent is different for both substrates. While for substrate **S1** the oxazoline group has little effect on enantioselectivity, being somewhat best with Ph or *i*-Pr oxazoline substituents (entries 3 and 6, ee's up to 96%), for the small unhindered substrate **S2**, a bulkier *t*-Bu group was needed to maximize enantioselectivity (entry 9, ee's up to 86%). These results contrast with the parent phosphite-oxazoline ligands **3**, where for both type of substrates the oxazoline substituent has

Table 1. Pd-catalyzed asymmetric allylic alkylation of **S1** and **S2** with ligands **L1**–**L3a**–**c**.[a]

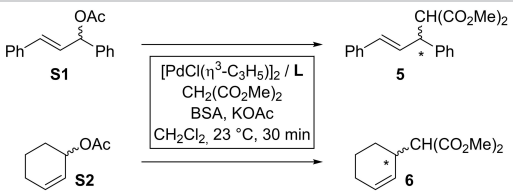

		5		6	
Entry	Ligand	%Conv[b]	% ee[c]	%Conv[b]	% ee[c]
1	**L1a**	100	92 (*S*)	100	60 (*R*)
2	**L1b**	100	86 (*S*)	100	51 (*R*)
3	**L1c**	100	95 (*S*)	100	66 (*S*)
4	**L2a**	100	89 (*S*)	100	40 (*R*)
5	**L2b**	100	82 (*S*)	100	30 (*R*)
6	**L2c**	100[d]	96 (*S*)[d]	100	48 (*S*)
7	**L3a**	100	73 (*S*)	100	30 (*R*)
8	**L3b**	100	72 (*S*)	100	80 (*R*)
9	**L3c**	100	92 (*S*)	100	86 (*S*)
10	**3**	100	>99 (*S*)[e]	100	99 (*S*)[e]
11	**4**	100	99 (*S*)[f]	100	99 (*S*)[f]

[a] 0.5 mol% $[PdCl(\eta^3\text{-}C_3H_5)]_2$, ligand (0.011 mmol), substrate (1 mmol), CH_2Cl_2 (2 mL), *N,O*-bis(trimethylsilyl)acetamide (BSA; 3 eq), dimethyl malonate (3 equiv), KOAc (3 mol%) at 23 °C. [b] Conversion percentage determined by ^{1}H-NMR spectroscopy after 30 min. [c] Enantiomeric excesses determined by HPLC or GC. Absolute configuration drawn in parentheses. [d] Reactions carried for 10 min using 0.1 mol% of catalyst precursor. TOF = 4048 mol **S1**$\times$(mol Pd$\times$h)$^{-1}$ measured after 5 min (68% conversion). [e] Data from Ref. [10b]. [f] Data from Ref. [8p].

Research Article
doi.org/10.1002/ejic.202100988

not effect on the achieved enantioselectivity. The consequence of introducing a methylene spacer between the oxazoline ring and the phenyl ring of ligands **3** is that the flexibility of the biaryl phosphite group alone is not able to adjust the size of the chiral pocket to the steric demands of the substrate. As a result, there is a complex interplay between the biaryl phosphite moiety and the nature of the oxazoline substituent that determines the enantioselectivity for each substrate type. Thus, while the best enantioselectivity for hindered linear substrate **S1** is obtained with **L2c**, for the cyclic substrate **S2** the use of **L3c** afforded the highest enantioselectivity.

In addition, the effect of the biaryl phosphite moiety on the catalytic performance is more pronounced in the cyclic substrate than in the linear one. Thus, while for **S1** the enantioselectivity varied from 82% (*S*) to 96% (*S*) by changing the configuration of the biaryl group due to a match/mismatch situation, for **S2** there was also an inversion in the configuration of the alkylation product (i.e. entries 8 vs 9).

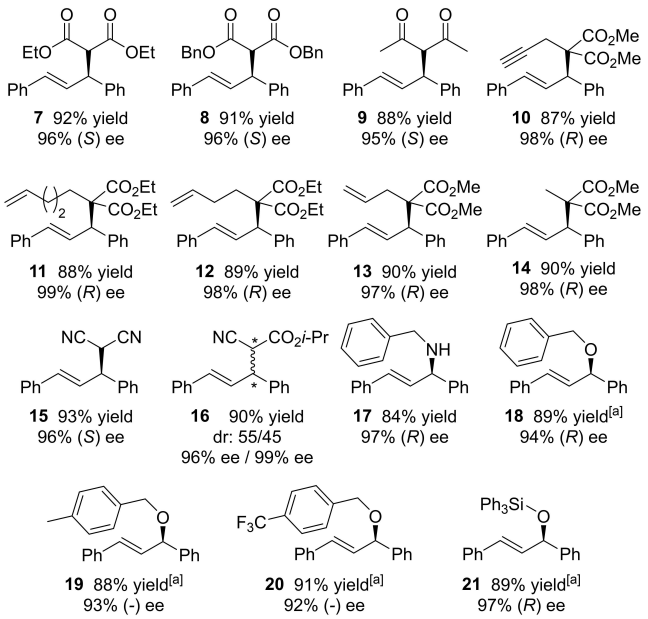

Figure 3. Pd-catalyzed allylic substitution of **S1** with Pd-**L2c** catalyst precursor using a range of C-, N- and O-nucleophiles. Reactions preformed in CH_2Cl_2 at 23 °C with $[PdCl(\eta^3\text{-}C_3H_5)]_2$ (0.5 mol%), ligand (1.1 mol%), BSA (3 equiv) and KOAc (3 mol%). Full conversions in 2 h.[a] Reactions carried out with 2 mol% $[PdCl(\eta^3\text{-}C_3H_5)]_2$, 4 mol% ligand and Cs_2CO_3 (3 equiv). Full conversions in 18 h.

Scope and limitations. Allylic substitution of different disubstituted substrates with a range of C-, N- and O-nucleophiles

We next investigated the scope of Pd/**L1**-**L3a**–**c** catalytic systems with other C-nucleophiles and with N- and O-nucleophiles, as well as testing linear and cyclic substrates with different steric and electronic requirements. We initially considered the allylic substitution of the benchmark **S1** substrate with a range of C-, N- and O-nucleophiles, including the more challenging functionalized malonates and alkyl alcohols (Figure 3). Positively several malonates, even those substituted with propargyl-, pentenyl-, butenyl-, and allyl groups, reacted with **S1** to offer products **7**, **8**, **10**–**14** in high yields and enantioselectivities up to 99%, even higher in some cases than those achieved with dimethyl malonate. These are important results since products **10**–**13** are key building blocks for the synthesis of fine molecules.[14] The reaction also performed well (ee's up to 96%) when the nucleophiles were acetylacetone (compound **9**) and malononitrile (compound **15**). As in previous publications the use of isopropyl cyanoacetate as nucleophile (compound **16**) give the formation of two diastereoisomers with low diastereoselectivity,[15] although both diastereoisomers were reached in high enantioselectivities (ee's up to 99%).

Enantiocontrol was also high when benzylamine was used as an example of N-nucleophile (compound **17**, 97% ee). Interestingly, enantioselectivities as high as those with dimethyl malonate were also found in the addition of several aliphatic alcohols and silanols (compounds **18**–**21**, ee's up to 97%). Aliphatic alcohols are another relevant set of nucleophiles whose resulting chiral ethers are found in biologically active targets.[16] Despite the extensive research dedicate to the addition of aliphatic alcohols very few effective catalysts exist whose enantioselectivities largely depends on the type of alcohol and its electronic properties.[17] Thus, for example with Pd/**3** system the enantioselectivity dropped considerable when electron rich benzylic alcohols were used.[10b] The reversed behavior was found with other Pd-catalysts.[8p,17c] Gratifyingly, the application of Pd/**L2c** in the etherification of **S1** with three aliphatic alcohols differing in their electronic properties, furnished the desired products in yields and enantioselectivities comparable to the best one reported so far. This represents an improvement regarding to the previously reported phosphite-based PHOX-ligands **3** and phosphite-oxazoline ligands **4**. High enantioselectivity were also reached with the triphenylsilanol as nucleophile (ee's up to 97%). As in previous publications a higher amount of Pd/L was required to achieve full conversions, due to the lower nucleophilicity of the aliphatic alcohols.

The results collected in Scheme 1 showed that Pd/**L2c** can also be successfully used for the alkylation of other symmetrical linear substrates **S3**–**S7** with steric and electronic requirements different from those of **S1**. High yields and enantioselectivities were therefore attained with a range of malonates including those substituted with propargyl, pentenyl and allyl groups (compounds **22**–**29**, ee's from 96% to 99%). Among these results, to highlight that Pd/**L2c** is also able to adapt its chiral cavity to highly sterically demanding substrates such as **S6** and **S7** (compounds **28** and **29**, ee's up to 99%).

We then studied the allylic substitution of cyclic substrate **S2** with more challenging nucleophiles than dimethyl malonate. We performed these studies with Pd/**L3c** catalytic system that provided the best results in the alkylation of **S2**. A wide range of C-nucleophiles, including acetylacetone and the less studied α-substituted malonates with propargyl, allyl and methyl groups, can react with **S2** to provide the desired corresponding compounds (**30**–**35**, Scheme 2) in high yields and enantioselec-

Research Article
doi.org/10.1002/ejic.202100988

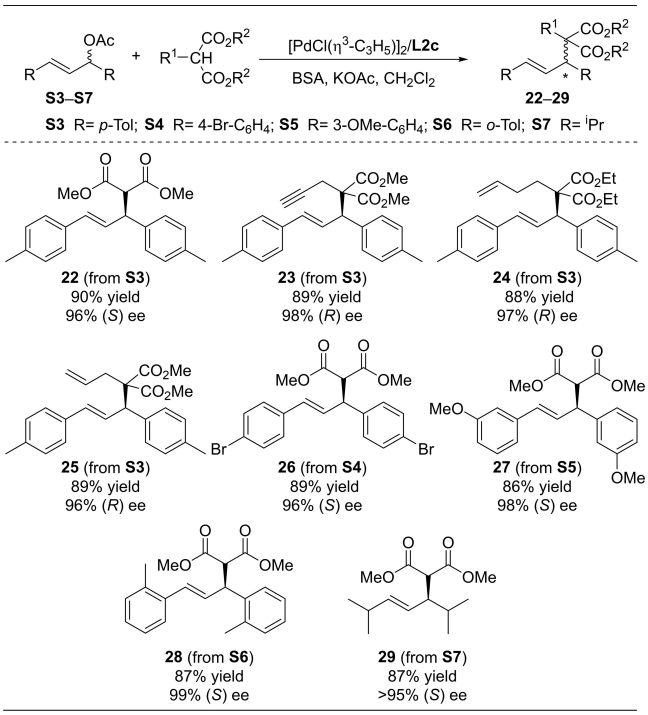

Scheme 1. Pd-catalyzed allylic substitution of **S3**–**S7** with C-nucleophiles using Pd/**L2c** catalytic system. Reactions were run at 23 °C with $[PdCl(\eta^3\text{-}C_3H_5)]_2$ (0.5 mol%), CH_2Cl_2 as solvent, ligand (1.1 mol%), BSA (3 equiv), and KOAc (3 equiv). Full conversions were achieved after 4 h.

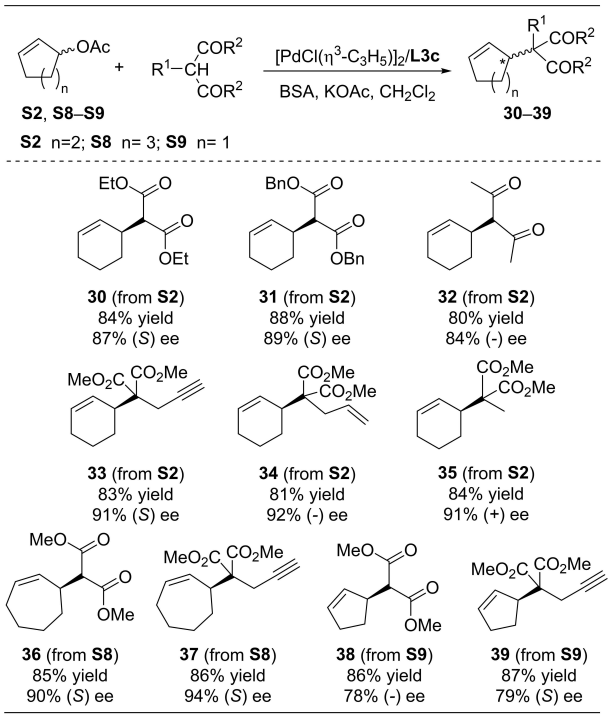

Scheme 2. Pd-catalyzed allylic alkylation of **S2**, **S8**–**S9** with the Pd/**L3c** catalyst precursor. Reactions were run at 23 °C with $[PdCl(\eta^3\text{-}C_3H_5)]_2$ (0.5 mol%), CH_2Cl_2 as solvent, ligand (1.1 mol%), BSA (3 equiv), and KOAc (3 equiv). Full conversions were achieved after 2 h.

tivities (ee's up to 92%), comparable to those achieved in the alkylation of **S2** with dimethyl malonate. Positively, Pd/**L3c** could also adjust its chiral pocket to cyclic substrates with higher (substrate **S8**) or lower (**S9**) ring sizes than **S2** (compounds **36**–**39**, ee's up to 94%), even using propargyl malonate as nucleophile. As for the cyclic substrate **S2**, for **S8** and **S9** there is an inversion of the configuration of the final product by using ligand **L3b**, with opposite configuration of the biaryl phosphite moiety (see Table SI-3).

Mechanistic studies. Origin of enantioselectivity

To better understand the effect of the ligand parameters on the enantioselectivities reached, we first performed a DFT study of the species involved in the nucleophilic attack, which is the enantiodetermining step. The transition state (TS) for this step, however, can be either early or late depending on the nucleophile, reaction conditions and ligands. In an early transition state, the enantioselectivity is controlled by both, the population of the Pd-η^3-allyl intermediates and the relative electrophilicity of the allylic carbon atoms, with an allyl terminus *trans* to a phosphorus atom being more reactive than one *trans* to a nitrogen in accordance with the stronger *trans* influence of the P atom.[18] For a late transition state the enantioselectivity is controlled by the Pd-olefin complex.[19]

The experimental catalytic results achieved with linear substrates show that the ligand parameter with the greatest effect on enantioselectivity is the chiral axis of the biaryl phosphite moiety. We therefore calculated the relative stability of the TSs and the Pd-olefin intermediates with the benchmark substrate **S1** with ligands **L2b** and **L2c** that differ only in the configuration of the biaryl phosphite moiety.[20] To accelerate the DFT calculations we used ammonia as nucleophile that also avoid the problems related to charge separation together with a continuum solvent model.[3,21] Note that the use of ammonia as nucleophile instead of dimethyl malonate results in the inversion of the CIP descriptor, due to the change in priority of the groups, although the sense of stereoselectivity is maintained. The results of most stable TSs ($TS_{exo\ (R)}$ and $TS_{endo\ (S)}$) and the most stable Pd − olefin complexes (Pd-$olefin_{exo(R)}$ and Pd-$olefin_{endo(S)}$) leading to the formation of both product enantiomers are shown in Table 2 (for the full set of calculated TSs and Pd–olefin complexes see Supporting information). The difference of energy of the calculated TSs with ligand **L2c** was higher ($\Delta G^{\neq} = 5.9$ kJ/mol; $ee_{calc} = 83\%$ (*R*)) than with **L2b** ($\Delta G = 4.2$ kJ/mol; $ee_{calc} = 69\%$ (*R*)), which match with the higher enantioselectivities found experimentally with **L2c**.

Moreover, the DFT correctly predicts the formation of the correct product enantiomer for both ligands. On the contrary, the predicted enantioselectivity of the Pd-olefin intermediates do not match with the experimental results. Although the calculations predict the formation of the correct product enantiomer for both ligands, a larger energy difference was found for the two Pd − olefin complexes with **L2b** ($\Delta G =$ 19.3 kJ/mol; $ee_{calc} > 99\%$ (*R*)) than for the two olefin complexes with **L2c** ($\Delta G = 3.1$ kJ/mol; $ee_{calc} = 55\%$ (*R*)). According to these

Research Article
doi.org/10.1002/ejic.202100988

Table 2. Schematic representation and relative free energies in solution of the most stable *exo*- and *endo*-transition states (in kJ/mol) (left) and of the most stable Pd-olefin complexes (right) for substrate **S1** with ammonia and ligands **L2b** and **L2c**.

Pd-TS		Pd-olefin	
L2b	L2c	L2b	L2c
$TS_{exo(R)}$ 0 kJ/mol	$TS_{exo(R)}$ 0 kJ/mol	Pd-olefin$_{exo(R)}$ 0 kJ/mol	Pd-olefin$_{exo(R)}$ 0 kJ/mol
$TS_{endo(S)}$ 4.2 kJ/mol	$TS_{endo(S)}$ 5.9 kJ/mol	Pd-olefin$_{endo(S)}$ 19.3 kJ/mol	Pd-olefin$_{endo(S)}$ 3.1 kJ/mol

values, **L2b** should provide a higher enantioselectivity than **L2c**, which does not agree with the enantioselectivities achieved experimentally.

In order to further support the DFT calculations, we prepared Pd-allyl complex **40** by reaction of the 1,3-diphenyl ally Pd chloride dimer with two equivalents of ligand **L2c**, followed by counterion exchange with $AgBF_4$ (Scheme 3a). The VT-NMR study showed a mixture of two isomers in equilibrium at a ca 4:1 ratio. As expected, NOE interactions indicated that these isomers corresponded to the *syn/syn exo* and *endo* intermediates, respectively (Scheme 3b). Thus, for both isomers there is a NOE interaction between the two terminal protons of the allyl group in agreement with a *syn/syn* disposition (Scheme 3c). In addition, for the major *exo* isomer there is an indicative NOE interaction between the terminal allylic proton *trans* to the P-moiety and the protons of one of the trimethylsilyl groups of the phosphite functionality that it is not present for the *endo* intermediate (Scheme 3c). The $^{13}C\{^1H\}$ NMR shifts of both isomers revealed that the most electrophilic allylic terminal carbons are found *trans* to the P-group. They also revealed that the terminal allylic carbon *trans* to P in the *exo* isomer is more electrophilic than the corresponding carbon for the *endo* isomer ($\Delta\delta(^{13}C) = 6.5$ ppm). This clearly indicates that the major *exo* isomer should react faster than the minor *endo* isomer, which is in line with the conclusions of the DFT calculations.[8k,n]

To find out the impact of the configuration of the biaryl phosphite group in the enantioselectivity we then examined, for each ligand, the structures of the two most stable TSs, leading to both enantiomers of the substituted product (Figure 4).

For both ligands the major product enantiomer comes from a TS with an *exo* disposition of the substrate, while the *endo* disposition is responsible for the minor enantiomer. It is also interesting to see that the *exo* TSs of both ligands adopt a "boat-chair" conformation of the eight-membered chelate ring (Figure 4). In addition, for both ligands the *exo* TSs are stabilized due to an strong attractive interaction between the H of the methine group of the oxazoline and one of the phenyl rings of the substrate (see the noncovalent interaction (NCI) plots, in blue, Figure 5).

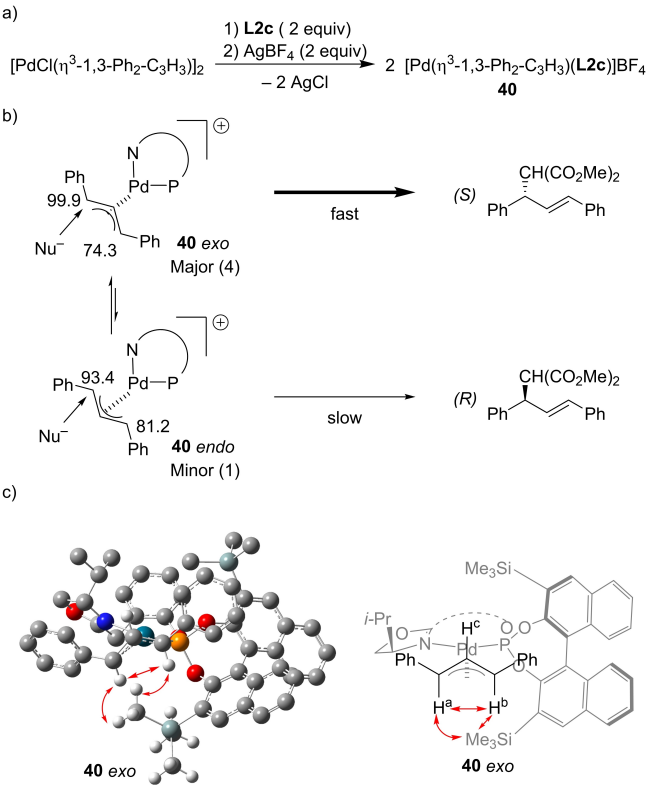

Scheme 3. a) Preparation of [Pd(η^3-1,3-Ph_2-C_3H_3)(**L2c**)]BF_4 **40**. b) Diastereoisomeric *exo* and *endo* Pd-η^3-allyl intermediates of complex **40**. The relative amounts of each isomer are shown in parentheses. The chemical shifts (in ppm) of the allylic terminal carbons are also shown. c) Calculated DFT structure for the major isomer of complex **40** (most of the hydrogen atoms have been omitted for clarity) and its schematic representation. Relevant NOE contacts that confirms its *exo* disposition are showed in red. H^a = terminal allyl proton *trans* to P; H^b = terminal allyl proton *trans* to N and H^c = central allyl proton.

The difference between both ligands becomes evident when we analyzed the structures of the *endo* TSs. The *endo* TS of ligand **L2b** still maintains a boat-chair conformation which is destabilized with respect to the *exo* boat-chair conformation for two main reasons. Firstly, the above-mentioned attractive CH/π interaction is weaker than in the *exo* TS and secondly there is a steric repulsion between one of the Ph rings of the substrate and the binaphthyl phosphite moiety. In contrast to ligand **L2b**, the *endo* TS of ligand **L2c** adopts a less stable "chair-chair" conformation (Figure 4). A TS with the same "boat-chair" disposition of the *endo* TS of ligand **L2b** is destabilized because the attractive CH/π interaction between the H from the oxazoline and the phenyl ring of the substrate does not exist because the H is pointing away from the coordination sphere (see Figure 6). Consequently, the ligand changes to a "chair-chair" conformation. This change of conformation increases the energy gap between the *endo* and the *exo* TSs and could explain the higher enantiomeric excess achieved with Pd/**L2c** over the Pd/**L2b**.

Research Article
doi.org/10.1002/ejic.202100988

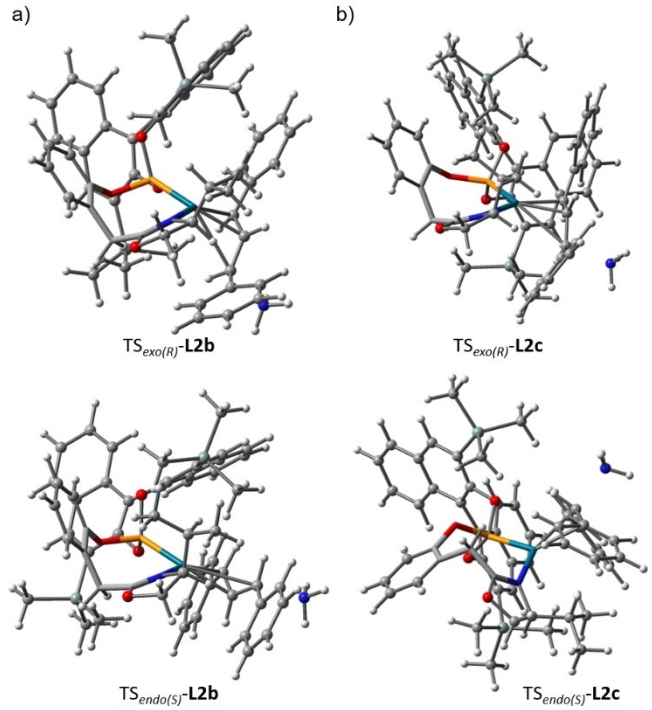

Figure 4. Most stable calculated TSs ($TS_{exo(R)}$ and $TS_{endo(S)}$) from **S1** using ligands (a) **L2b** and (b) **L2c**. The eight-membered chelate ring is highlighted using capped sticks, while the rest of the TS is shown using balls and sticks.

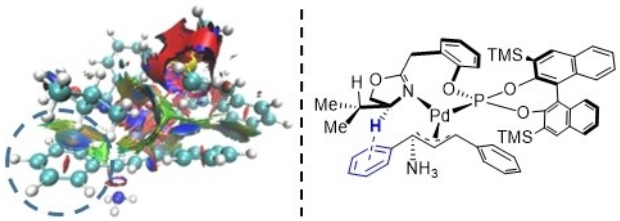

Figure 5. NCI plot of $TS_{exo(R)}$ with ligand **L2b** showing the CH/π interaction between the H of the methine group of the oxazoline and one of the phenyl rings of the substrate. NCIs were measured constructing the isosurface with the Multiwfn software, which were visualized with VMD.

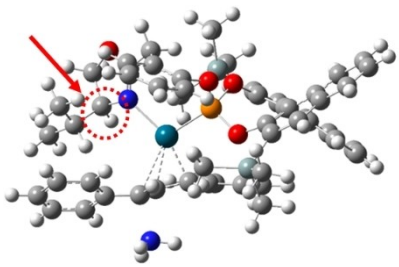

Figure 6. Calculated geometry for $TS_{endo(R)}$ using ligand **L2c**. The H of the methine group of the oxazoline is highlighted in red.

To shed some light on the different behavior of the allylic substitution of cyclic substrates, for which the enantioselectivity varied from 80% of the *R*-enantiomer (ligand **L3b**) to 86% of the *S*-enantiomer (ligand **L3c**) when the configuration of the biaryl phosphite group was changed, we studied the intermediate Pd-allyl complexes **41** and **42** (Scheme 4).

For complex **41**, containing ligand **L3c** and a biaryl group with *S* configuration, two isomers were detected by NMR with ratio 1.2:1 (Scheme 5a). The NOESY spectrum indicated an *endo* disposition for the major isomer (responsible for the *S*-product) and an *exo* disposition for the minor (responsible for the *R*-product). For the minor isomer the *t*-butyl oxazoline group has NOE interactions with the terminal allyl proton *trans* to the phosphite group and also with the central allyl proton, whereas for the major *endo* isomer the central allyl proton showed a NOE interaction with one of the trimethyl silyl groups (TMS) of the phosphite group (Figure SI-10). The large difference on the chemical shifts of the allylic carbon *trans* to the phosphite group ($\Delta(^{13}C) = 6.7$ ppm) indicates that the major isomer reacts faster than the minor one, leading to observed preferential formation of the *S*-enantiomer.

For complex **42** containing ligand **L3b** and a biaryl group with *R* configuration, only one isomer was found, whose NOE confirmed an *exo* disposition (Scheme 5b). As for the minor isomer of Pd/**L3c**, the NOE showed interactions of the *tert*-butyl oxazoline group with the terminal allyl proton *trans* to the

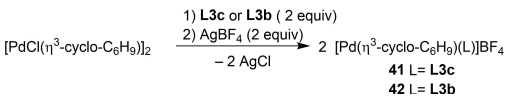

Scheme 4. Synthesis of $[Pd(\eta^3\text{-cyclo-}C_6H_9)(L)]BF_4$ complexes **41** and **42**.

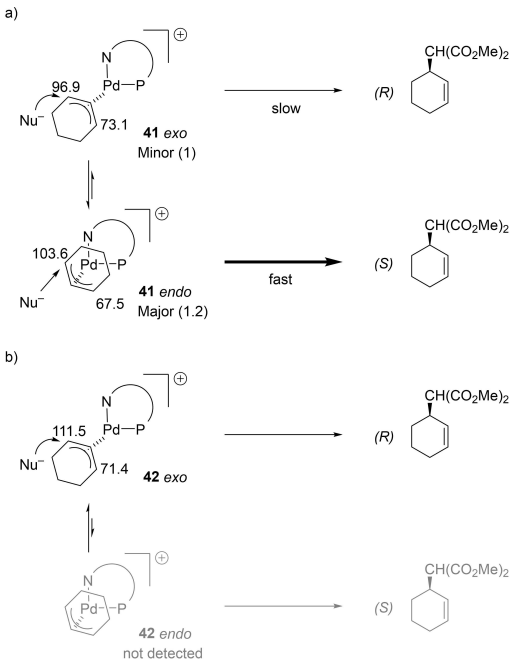

Scheme 5. Diastereoisomeric *exo* and *endo* Pd-η^3-allyl intermediates of: a) complex **41** and b) complex **42**. The relative amounts of each isomer are shown in parentheses. The chemical shifts (in ppm) of the allylic terminal carbons are also shown.

Research Article
doi.org/10.1002/ejic.202100988

phosphite group and also with the central allyl proton (Figure SI-15).

In summary, the configuration of the biaryl group affects which isomer is preferentially formed with ligands **L3b** and **L3c**. The *exo* isomer is favored with ligands with an *R*-configuration of the biaryl moiety, while ligands with the opposite configuration favor the formation of the *endo* isomer.

The different effect of the configuration of the biaryl phosphite moiety on the outcome of the allylic substitution with linear and cyclic substrates can be explained by the different substrate geometry and the relative position of the trimethylsilyl groups of the biaryl phosphite group. Thus, in Figure 4 we can see that one of the TMS moiety are located above or below the Pd atom and in the space of the substrate coordination, depending on the configuration of the biaryl phosphite group. This feature is clearly illustrated in Figure 7a, where an apical view of the two *endo* TSs (TS_{endo}-**L2b** and TS_{endo}-**L2c**) is presented. In both cases one of the TMS groups is located almost at the same axis as the Pd atom, whereas the other TMS is located far from the substrate coordination sphere. However, whereas for the TS_{endo}-**L2b** the TMS group is located above the Pd atom, for the TS_{endo}-**L2c** the TMS group is located below the Pd atom. This disposition of the TMS groups has a small effect in favoring one of the two isomers (either *endo* or *exo*) for the linear substrate since the phenyl groups of the substrate are located far from the metal center and therefore far from the TMS group (Figure 7b). However, for the cyclic substrates the arrangement of the TMS group above or below to the Pd, has a direct effect in which of the two isomers is predominant (Figure 7c).

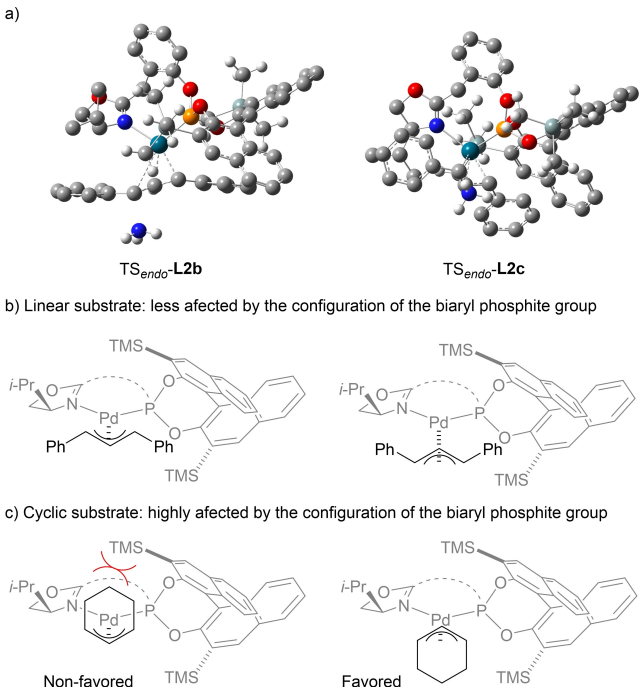

Figure 7. a) Apical view of the *endo* TSs with ligands **L2b** and **L2c**. Most of the hydrogen atoms except those of the TMS groups have been omitted for clarity. Steric environment found in *endo* and *exo* isomers in Pd/**L2b**-allyl complexes containing an *R*-biaryl phosphite moiety as example with: b) substrate **S1** and c) substrate **S2**.

Conclusion

A small library of air stable phosphite-oxazoline ligands has been tested in Pd-catalyzed allylic substitutions of a wide range of substrate types and nucleophiles (35 compounds in total), with high enantioselectivities (up to 99%) and activities (TOF's up to $>4000\ h^{-1}$). These ligands, which are readily available in only two synthetic steps, are derived from the PHOX ligand by replacing the phosphine moiety by biaryl phosphites and by introducing a methylene spacer between the oxazoline and the phenyl ring. These simple modifications allowed to increase the substrate and nucleophile scope of the PHOX ligands. We identified two ligands with good performance for a range of hindered (ligands **L2c**) and cyclic substrates (ligand **L3c**), with several nucleophiles. The two ligands have in common a chiral *S* biaryl phosphite moiety and differ at the oxazoline moiety. Mechanistic studies based on DFT calculations and NMR spectroscopy of the key Pd-intermediates allowed us to better understand the origin of the enantioselectivities. The wide substrate scope found is due to the ability of the ligand to adapt their ligand parameters to the reacting substrate. This contrasts to the parent phosphite-oxazoline ligands **3**. In this respect, while for hindered linear substrate the enantioselectivity is mainly affected by the biaryl phosphite functionality and therefore by the conformation adopted by the chelate ring, for the cyclic substrate the oxazoline group also has a crucial role. Accordingly a bulky oxazoline group is needed to adapt the size of the substrate binding pocket to the narrow substrate. In addition, the higher effect of the configuration of the biaryl phosphite moiety on the catalytic performance in cyclic substrates can be explained by the relative disposition of the trimethylsilyl groups of the biaryl phosphite moiety and their interactions with the substrates. These results open up the use of solid, air stable and readily available ligands to advance in the Pd-AAS of several substrate types with diverse nucleophiles.

Experimental Section

General Procedures. All reactions were carried out using standard Schlenk techniques under an argon atmosphere. Commercial chemicals were used as received. Solvents were dried by means of standard procedures and stored under argon. ^{1}H, $^{13}C\{^{1}H\}$ and $^{31}P\{^{1}H\}$ NMR spectra were recorded using a Varian Mercury-400 MHz spectrometer. Chemical shifts are relative to that of NMR solvent for ^{1}H and $^{13}C\{^{1}H\}$ and of H_3PO_4 as internal standard for $^{31}P\{^{1}H\}$. The referenced $^{31}P\{^{1}H\}$ spectra in the Supporting Information are displayed without the internal standard. Racemic substrates **S1**-**S9**[22] and ligands **L1**–**L3a**–**c**[12a,b] were prepared as previously reported.

Typical procedure for the allylic alkylation reactions. A degassed solution of $[PdCl(\eta^3\text{-}C_3H_5)]_2$ (1.8 mg, 0.005 mmol) and the desired phosphite-oxazoline ligand (0.011 mmol) in dichloromethane (0.5 mL) was stirred for 30 min. After this time, a solution of substrate (1 mmol) in dichloromethane (1.5 mL), nucleophile

(3 mmol), *N*,*O*-bis(trimethylsilyl)-acetamide (3 mmol) and KOAc (3 mg, 0.03 mmol) were added. The reaction mixture was stirred at room temperature. After the desired reaction time the reaction mixture was diluted with Et_2O (5 mL) and saturated NH_4Cl (aq) (25 mL) was added. The mixture was extracted with Et_2O (3×10 mL) and the extract dried over $MgSO_4$. For compounds **5**, **7–16**, **22–28**, **32–33** and **37**, the solvent was removed, conversions were measured by ^1H NMR and enantiomeric excesses were determined by HPLC. For compounds **6**, **30–31**, **34–36** and **39**, conversion and enantiomeric excesses were determined by GC. For compounds **29** and **38**, conversion was measured by ^1H NMR and ee's were determined by ^1H NMR using [Eu(hfc)$_3$]. Characterization and enantiomeric excess determination details can be found in the Supporting Information.

Typical* procedure *for the allylic amination of S1. A degassed solution of $[PdCl(\eta^3\text{-}C_3H_5)]_2$ (1.8 mg, 0.005 mmol) and the desired phosphite-oxazoline ligand (0.011 mmol) in dichloromethane (0.5 mL) was stirred for 30 min. After this time, a solution of substrate (1 mmol) in dichloromethane (1.5 mL) and benzylamine (262 μL, 3 mmol) were added. The reaction mixture was stirred at room temperature. After the desired reaction time the reaction mixture was diluted with Et_2O (5 mL) and saturated NH_4Cl (aq) (25 mL) was added. The mixture was extracted with Et_2O (3×10 mL) and the extract dried over $MgSO_4$. Conversion was measured by ^1H NMR and enantiomeric excesses of compound **17** were determined by HPLC. Characterization and enantiomeric excess determination details can be found in the Supporting Information.

Typical procedure for the allylic etherification and silylation of S1. A degassed solution of $[PdCl(\eta^3\text{-}C_3H_5)]_2$ (1.8 mg, 0.005 mmol) and the desired phosphite-oxazoline ligand (0.011 mmol) in dichloromethane (0.5 mL) was stirred for 30 min. Subsequently, a solution of **S1** (31.5 mg, 0.125 mmol) in dichloromethane (1.5 mL) was added. After 10 min, Cs_2CO_3 (122 mg, 0.375 mmol) and the corresponding alkyl alcohol or silanol (0.375 mmol) were added. The reaction mixture was stirred at room temperature. After the desired reaction time, the reaction mixture was diluted with Et_2O (5 mL) and saturated NH_4Cl (aq) (25 mL) was added. The mixture was extracted with Et_2O (3×10 mL) and the extract dried over $MgSO_4$. Conversions were measured by ^1H NMR and enantiomeric excesses for compounds **18–21** were determined by HPLC. Characterization and enantiomeric excess determination details can be found in the Supporting Information.

Computational details. The geometries of all intermediates were optimized using the Gaussian 09 program,[23] employing the B3LYP[24] density functional and the LANL2DZ[25] basis set for palladium and the 6–31G* basis set for all other elements.[26] Solvation correction was applied in the course of the optimizations using the PCM model with the default parameters for dichloromethane.[27] The complexes were treated with charge +1 and in the single state. No symmetry constraints were applied. The energies were further refined by performing single point calculations using the above mentioned parameters, with the exception that the 6–311+G**[28] basis set was used for all elements except palladium, and by applying dispersion correction using DFT–D3[29] model. All energies reported are Gibbs free energies at 298.15 K and calculated as $G_{reported} = G_{6\text{-}31G^*} + (E_{6\text{-}311+G^{**}} - E_{6\text{-}31G^*}) + E_{DFT\text{-}D3}$.

We used the NCI method[30] to study the non-covalent interactions. The method is capable of mapping real-space regions where non-covalent interactions are important and is based exclusively on the electron density and its gradient. The information provided by NCI plots is essentially qualitative. To perform these calculations, we used promolecular approximation using xyz files.

Typical procedure for the preparation of [Pd(η³-allyl)(L)]BF₄ complexes 40–42. The corresponding ligand (0.05 mmol) and the complex $[Pd(\mu\text{-}Cl)(\eta^3\text{-}1,3\text{-allyl})]_2$ (0.025 mmol) were dissolved in CD_2Cl_2 (1.5 mL) at room temperature under argon. $AgBF_4$ (9.8 mg, 0.05 mmol) was added after 30 minutes and the mixture was stirred for other 30 minutes more. The mixture was then filtered over celite under argon and the resulting solutions were analyzed by NMR.

[Pd(η³-1,3-Ph$_2$-C$_3$H$_3$)(L2c)]BF$_4$ complex 40. Major isomer: $^{31}P\{^1H\}$ NMR (161.9 MHz, CD_2Cl_2): δ = 132.9 (s). ^1H NMR (400 MHz, CD_2Cl_2): δ = 0.44 (s, 9H, CH_3–Si), 0.62 (s, 9H, CH_3–Si), 0.70 (m, 6H, CH_3, *i*-Pr), 1.65 (m, 1H, CH, *i*-Pr), 2.48 (m, 1H, CH–N), 3.78 (d, 1H, CH_2, $^2J_{H\text{-}H}$ = 14.8 Hz), 3.92–4.15 (m, 2H, CH_2–O), 4.35 (d, 1H, CH_2, $^2J_{H\text{-}H}$ = 14.8 Hz), 4.77 (d, 1H, CH=trans to N, *J* = 11.2 Hz), 5.81 (m, 1H, CH=trans to P), 6.21 (m, 2H, CH=), 6.60 (m, 2H, CH=), 6.83 (m, 2H, CH=central and CH=), 6.92–8.32 (m, 19H, CH=). $^{13}C\{^1H\}$ (100.6 MHz, CD_2Cl_2): δ = 0.3 (CH_3, $SiMe_3$), 0.7 (CH_3, $SiMe_3$), 16.2 (CH_3, *i*-Pr), 18.9 (CH_3, *i*-Pr), 31.4 (CH, *i*-Pr), 35.1 (CH_2), 67.2 (CH–N), 70.6 (CH_2–O), 74.3 (d, CH=*trans* to N, $J_{C\text{-}P}$ = 7.6 Hz), 99.9 (d, CH=*trans* to P, $J_{C\text{-}P}$ = 33.0 Hz), 110.7 (d, CH=central, $J_{C\text{-}P}$ = 10.4 Hz), 126.2–151.4 (aromatic carbons), 169.8 (C=N). Minor isomer: $^{31}P\{^1H\}$ NMR (161.9 MHz, CD_2Cl_2): δ = 134.4 (s). ^1H NMR (400 MHz, CD_2Cl_2): δ = 0.31 (s, 9H, CH_3–Si), 0.48 (s, 9H, CH_3–Si), 0.70 (m, 3H, CH_3, *i*-Pr), 0.86 (m, 3H, CH_3, *i*-Pr), 1.89 (m, 1H, CH, *i*-Pr), 2.27 (m, 1H, CH–N), 3.54 (d, 1H, CH_2, $^2J_{H\text{-}H}$ = 13.6 Hz), 3.92–4.15 (m, 2H, CH_2–O), 4.09 (m, 1H, CH_2), 5.27 (d, 1H, CH=trans to N, *J* = 12 Hz), 5.44 (m, 1H, CH=trans to P), 6.38 (m, 2H, CH=), 6.65 (m, 1H, CH=), 6.83 (m, 2H, CH=central and 2×CH=), 6.92–8.32 (m, 19H, CH=). $^{13}C\{^1H\}$ (100.6 MHz, CD_2Cl_2): δ = −0.4 (CH_3, $SiMe_3$), −0.1 (CH_3, $SiMe_3$), 15.5 (CH_3, *i*-Pr), 18.0 (CH_3, *i*-Pr), 31.0 (CH, *i*-Pr), 34.7 (CH_2), 69.1 (CH–N), 69.7 (CH_2–O), 81.2 (d, CH=*trans* to N, $J_{C\text{-}P}$ = 5.9 Hz), 93.4 (d, CH=*trans* to P, $J_{C\text{-}P}$ = 40.5 Hz), 112.4 (d, CH=central, $J_{C\text{-}P}$ = 12.6 Hz), 126.2–151.4 (aromatic carbons), 169.9 (C=N).

[Pd(η³-cyclo-C$_6$H$_9$)(L3c)]BF$_4$ complex 41. Major isomer: $^{31}P\{^1H\}$ NMR (161.9 MHz, CD_2Cl_2): δ = 134.7 (s). ^1H NMR (400 MHz, CD_2Cl_2): δ = 0.32 (s, 9H, CH_3–Si), 0.57 (s, 9H, CH_3–Si), 0.99 (m, 9H, CH_3, *t*-Bu), 1.1–2.2 (b, 5H, CH_2), 2.49 (m, 1H, CH_2), 3.71 (d, 1H, CH_2, $^2J_{H\text{-}H}$ = 14.4 Hz), 3.80 (d, 1H, CH_2, $^2J_{H\text{-}H}$ = 14.4 Hz), 3.97 (b, 1H, CH=trans to N), 4.03 (dd, 1H, CH–N, *J* = 9.6 Hz, *J* = 3.2 Hz), 4.64 (m, 2H, CH_2–O), 5.50 (b, 1H, CH=central), 6.36 (b, 1H, CH=trans to P), 6.12–8.30 (m, 14H, CH=).$^{13}C\{^1H\}$ (100.6 MHz, CD_2Cl_2): δ = 0.0 (2xCH_3, $SiMe_3$), 20.3 (CH_2), 25.9 (CH_3, *t*-Bu), 26.6 (CH_2), 28.2 (d, CH_2, $J_{C\text{-}P}$ = 8.3 Hz), 29.1 (C, *t*-Bu), 34.8 (d, CH_2, $J_{C\text{-}P}$ = 10.2 Hz), 67.5 (b, CH=*trans* to N), 71.7 (CH_2–O), 78.2 (CH–N), 103.6 (d, CH=*trans* to P, $J_{C\text{-}P}$ = 42.5 Hz), 112.7 (d, CH=central, $J_{C\text{-}P}$ = 11.4 Hz), 120.8–151.4 (aromatic carbons), 169.8 (C=N). Minor isomer: $^{31}P\{^1H\}$ NMR (161.9 MHz, CD_2Cl_2): δ = 135.0 (s). ^1H NMR (400 MHz, CD_2Cl_2): δ = 0.43 (s, 9H, CH_3–Si), 0.52 (s, 9H, CH_3–Si), 0.90 (m, 9H, CH_3, *t*-Bu), 1.1–2.2 (b, 6H, CH_2), 4.15 (dd, 1H, CH–N, *J* = 9.6 Hz, *J* = 4.4 Hz), 4.47 (dd, 1H, CH_2, $^2J_{H\text{-}H}$ = 14.4 Hz, *J* = 2.4 Hz), 4.52 (m, 2H, CH_2–O), 5.10 (b, 1H, CH=trans to N), 5.70 (b, 1H, CH=central), 6.29 (b, 1H, CH=trans to P), 6.12–8.30 (m, 14H, CH=).$^{13}C\{^1H\}$ (100.6 MHz, CD_2Cl_2): δ = 0.2 (CH_3, $SiMe_3$), 0.5 (CH_3, $SiMe_3$), 16.9 (CH_2), 25.6 (CH_3, *t*-Bu), 28.7 (CH_2), 29.1 (C, *t*-Bu), 29.8 (d, CH_2, $J_{C\text{-}P}$ = 9.1 Hz), 35.9 (d, CH_2, $J_{C\text{-}P}$ = 10.2 Hz), 71.4 (CH_2–O), 73.1 (b, CH=*trans* to N), 77.3 (CH–N), 96.9 (d, CH=*trans* to P, $J_{C\text{-}P}$ = 31.2 Hz), 114.8 (d, CH=central, $J_{C\text{-}P}$ = 9.9 Hz), 120.8–151.4 (aromatic carbons), 171.0 (C=N).

[Pd(η³-1,3-cyclo-C$_6$H$_9$)(L3b)]BF$_4$ complex 42. $^{31}P\{^1H\}$ NMR (161.9 MHz, CD_2Cl_2): δ = 142.4 (s). ^1H NMR (400 MHz, CD_2Cl_2): δ = 0.06 (s, 9H, CH_3–Si), 0.32 (s, 9H, CH_3–Si), 0.48 (s, 9H, CH_3, *t*-Bu), 0.75 (m, 1H, CH_2), 0.89 (m, 1H, CH_2), 1.42 (m, 1H, CH_2), 1.56 (m, 1H, CH_2), 1.75 (b, 2H, CH_2), 3.17 (m, 1H, CH=trans to N), 3.62 (d, 1H, CH_2, $^2J_{H\text{-}H}$ = 14.4 Hz), 3.87 (m, 1H, CH–N), 4.22 (d, 1H, CH_2, $^2J_{H\text{-}H}$ = 14.4 Hz), 4.38 (m, 2H, CH_2–O), 5.03 (m, 1H, CH=central), 6.07 (m, 1H, CH=trans to P), 6.81–7.38 (m, 10H, CH=), 7.82–7.84 (m, 2H, CH=), 8.01–8.03 (m, 2H, CH=). $^{13}C\{^1H\}$ (100.6 MHz, CD_2Cl_2): δ = 0.2 (CH_3, $SiMe_3$), 1.1 (CH_3, $SiMe_3$), 19.8 (CH_2), 25.6 (CH_3, *t*-Bu), 26.9 (CH_2 and C, *t*-Bu), 28.4

(d, CH_2, $J_{C\text{-}P}$ = 7.6 Hz), 35.1 (CH_2), 70.6 (CH_2–O), 71.4 (b, CH=*trans* to N), 79.7 (CH–N), 111.1 (d, CH=central, $J_{C\text{-}P}$ = 33.4 Hz), 111.5 (d, CH=*trans* to P, $J_{C\text{-}P}$ = 9.1 Hz), 121.4–157.1 (aromatic carbons), 174.6 (C=N).

Acknowledgements

Grant PID2019-104904GB-I00 funded by MCIN/AEI/10.13039/501100011033 and grant 2017SGR1472 funded by the Catalan Government are gratefully acknowledged. Dr. M. Besora is gratefully acknowledged for her help in the supervision of DFT calculations.

Conflict of Interest

The authors declare no conflict of interest.

Data Availability Statement

The data that support the findings of this study are available in the supplementary material of this article.

Keywords: Palladium · Allylic substitution · Asymmetric catalysis · P,N-ligands · Mechanistic investigation

[1] See for example: a) O. Pàmies, J. Margalef, S. Cañellas, J. James, E. Judge, P. J. Guiry, C. Moberg, J.-E. Bäckvall, A. Pfaltz, M. A. Pericàs, M. Diéguez, *Chem. Rev.* **2021**, *121*, 4373–4505; b) H.-M. Huang, P. Bellotti, F. Glorius, *Chem. Soc. Rev.* **2020**, *49*, 6186–6197; c) Z. Lu, S. Ma, *Angew. Chem. Int. Ed.* **2008**, *47*, 258–297; *Angew. Chem.* **2008**, *120*, 264–303; d) E. Yoshioka, S. Kohtani, H. Miyabe, *Trends in Heterocyclic Chemistry* **2009**, *14*, 1–16; e) B. M. Trost, T. Zhang, J. D. Sieber, *Chem. Sci.* **2010**, *1*, 427–440; f) B. M. Trost, *Org. Process Res. Dev.* **2012**, *16*, 185–194; g) *Transition Metal Catalyzed Enantioselective Allylic Substitution in Organic Synthesis* (Ed.: U. Kazmaier), Springer, Cham, **2012**; h) C. Kammerer, G. Prestat, D. Madec, G. Poli, *Acc. Chem. Res.* **2014**, *47*, 3439–3447; i) N. A. Butta, W. Zhang, *Chem. Soc. Rev.* **2015**, *44*, 7929–7967; j) R. L. Grange, E. A. Clizbe, P. A. Evans, *Synthesis* **2016**, *48*, 2911–2968; k) N. Butt, G. Yang, W. Zhang, *Chem. Rec.* **2016**, *16*, 2687–2696.

[2] a) B. M. Trost, D. L. van Vranken, C. Bingel, *J. Am. Chem. Soc.* **1992**, *114*, 9327–9343; b) B. M. Trost, *Acc. Chem. Res.* **1996**, *29*, 355–364; c) B. M. Trost, R. C. Bunt, *J. Am. Chem. Soc.* **1994**, *116*, 4089–4090; d) B. M. Trost, A. C. Krueger, R. C. Bunt, J. Zambrano, *J. Am. Chem. Soc.* **1996**, *118*, 6520–6521.

[3] C. P. Butts, E. Filali, G. C. Lloyd-Jones, P.-O. Norrby, D. A. Sale, Y. Schramm, *J. Am. Chem. Soc.* **2009**, *131*, 9945–9957.

[4] G. Mata, C. A. Kalnmals, *Isr. J. Chem.* **2021**, *61*, 427–468 and references there in.

[5] a) P. von Matt, A. Pfaltz, *Angew. Chem. Int. Ed.* **1993**, *32*, 566–568; *Angew. Chem.* **1993**, *105*, 614–615; b) J. Sprinz, G. Helmchen, *Tetrahedron Lett.* **1993**, *34*, 1769–1772; c) G. J. Dawson, C. G. Frost, J. M. J. Williams, S. J. Coote, *Tetrahedron Lett.* **1993**, *34*, 3149–3150; d) G. Helmchen, A. Pfaltz, *Acc. Chem. Res.* **2000**, *33*, 336–345.

[6] a) *Privileged Chiral Ligands and Catalysts* (Ed.: Q.-L. Zhou), Wiley-VCH, Weinheim, **2011**; b) W. Sommer, D. Weibel, *Sigma Aldrich's Chemfiles* **2008**, *2*, 1–91.

[7] a) *Chiral ligands. Evolution of ligand libraries for asymmetric catalysis* (Ed.: M. Diéguez), CRC Press, Boca Raton, **2021**; b) J. Margalef, M. Biosca, P. De la Cruz-Sánchez, J. Faiges, O. Pàmies, M. Diéguez, *Coord. Chem. Rev.* **2021**, *446*, 214120.

[8] For selected papers on Pd-catalyzed allylic substitution reaction see: a) Q.-F. Wang, W. He, X.-Y. Liu, H. Chen, X.–Y. Qin, S.-Y. Zhang, *Tetrahedron: Asymmetry* **2008**, *19*, 2447–2450; b) H. Y. Cheung, W.-Y. Yu, T. T. L. Au-Yeung, Z. Zhou, A. S. C. Chan, *Adv. Synth. Catal.* **2009**, *351*, 1412–1422; c) H.-G. Cheng, B. Feng, L.-Y. Chen, W. Guo, X.-Y. Yu, L.-Q. Lu, J.-R. Chen, W.-J. Xiao, *Chem. Commun.* **2014**, *50*, 2873–2875; d) Z. Qiu, R. Sun, D. Teng, *Org. Biomol. Chem.* **2018**, *16*, 7717–7724; e) T. Noël, K. Bert, E. Van der Eycken, J. Van der Eycken, *Eur. J. Org. Chem.* **2010**, 4056–4061; f) Q.-L. Liu, W. Chen, Q.-Y. Jiang, X.-F. Bai, Z. Li, Z. Xu, L.-W. Xu, *ChemCatChem* **2016**, *8*, 1495–1499; g) T. Nemoto, M. Kanematsu, S. Tamura, Y. Hamada, *Adv. Synth. Catal.* **2009**, *351*, 1773–1778; h) B. Lu, B. Feng, H. Ye, J.-R. Chen, W.-J. Xiao, *Org. Lett.* **2018**, *20*, 3473–3476; i) C. Borràs, P. Elías-Rodríguez, A. T. Carmona, I. Robina, O. Pàmies, M. Diéguez, *Organometallics* **2018**, *37*, 1682–1694; j) J. Margalef, M. Coll, P.-O. Norrby, O. Pàmies, M. Diéguez, *Organometallics* **2016**, *35*, 3323–3335; k) Y. Mata, O. Pàmies, M. Diéguez, *Adv. Synth. Catal.* **2009**, *351*, 3217–3234; l) J. Mazuela, A. Paptchikhine, P. Tolstoy, O. Pàmies, M. Diéguez, P. G. Andersson, *Chem. Eur. J.* **2010**, *16*, 620–638; m) J. Mazuela, O. Pàmies, M. Diéguez, *Chem. Eur. J.* **2013**, *19*, 2416–2432; n) M. Magre, M. Biosca, P.-O. Norrby, O. Pàmies, M. Diéguez, *ChemCatChem.* **2015**, *7*, 4091–4107; o) M. Biosca, J. Margalef, X. Caldentey, M. Besora, C. Rodríguez-Escrich, J. Saltó, X. C. Cambeiro, F. Maseras, O. Pàmies, M. Diéguez, *ACS Catal.* **2018**, *8*, 3587–3601; p) M. Biosca, J. Saltó, M. Magre, P.-O. Norrby, O. Pàmies, M. Diéguez, *ACS Catal.* **2019**, *9*, 6033–6048.

[9] a) M. Diéguez, O. Pàmies, *Acc. Chem. Res.* **2010**, *43*, 312–322; b) P. W. N. M. Van Leeuwen, P. C. J. Kamer, C. Claver, O. Pàmies, M. Diéguez, *Chem. Rev.* **2011**, *111*, 2077–2118; c) O. Pàmies, M. Diéguez, *Chem. Rec.* **2016**, *16*, 2460–2481; d) M. Diéguez, O. Pàmies, C. Moberg, *Acc. Chem. Res.* **2021**, *54*, 3252–3263.

[10] a) O. Pàmies, M. Diéguez, C. Claver, *J. Am. Chem. Soc.* **2005**, *127*, 3646–3647; b) R. Bellini, M. Magre, M. Biosca, P.-O. Norrby, O. Pàmies, M. Diéguez, C. Moberg, *ACS Catal.* **2016**, *6*, 1701–1712.

[11] J. Margalef, O. Pàmies, M. A. Pericàs, M. Diéguez, *Chem. Commun.* **2020**, *56*, 10795–10808.

[12] a) M. Magre, O. Pàmies, M. Diéguez, *ACS Catal.* **2016**, *6*, 5186–5190; b) M. Biosca, M. Magre, M. Coll, O. Pàmies, M. Diéguez, *Adv. Synth. Catal.* **2017**, *359*, 2801–2814; c) Z. Mazloomi, M. Magre, E. Del Valle, M. A. Pericàs, O. Pàmies, P. W. N. M. van Leeuwen, M. Diéguez, *Adv. Synth. Catal.* **2018**, *360*, 1650–1664.

[13] We also studied the effect of Pd/L ratio. No effect on the catalytic performance was observed, see Supporting Information for details.

[14] See for example: a) J. Dugal-Tessier, G. R. Dake, D. P. Gates, *Org. Lett.* **2010**, *12*, 4667–4669; b) Y. Nakai, Y. Uozumi, *Org. Lett.* **2005**, *7*, 291–293; c) S. U. Son, K. H. Park, H. Seo, Y. K. Chung, S.-G. Lee, *Chem. Commun.* **2001**, 2440–2441; d) A. Farwick, J. U. Engelhart, O. Tverskoy, C. Welter, Q. E. Umlauf, F. Rominger, W. J. WillKerr, G. Helmchen, *Adv. Synth. Catal.* **2011**, *353*, 349–370; e) M. Biosca, J. Margalef, X. Caldentey, M. Besora, C. Rodríguez-Escrich, J. Saltó, X. C. Cambeiro, F. Maseras, O. Pàmies, M. Diéguez, M. A. Pericàs, *ACS Catal.* **2018**, *8*, 3587–3601.

[15] a) I. Kmentov, B. Gotov, E. Solcniov, S. Toma, *Green Chem.* **2002**, *4*, 103–106; b) J. Liu, G. Chen, J. Xing, J. Liao, *Tetrahedron: Asymmetry* **2011**, *22*, 575–579; c) Y. Jin, D. M. Du, *Tetrahedron* **2012**, *68*, 3633–3640; d) C. J. Martin, D. J. Rawson, J. M. J. Williams, *Tetrahedron: Asymmetry* **1998**, *9*, 3723–3730; e) W. H. Deng, F. Ye, X. F. Bai, Z. J. Zheng, Y. M. Cui, L. W. Xu, *ChemCatChem* **2015**, *7*, 75–79.

[16] a) *Dictionary of Natural Products*, (Ed.: J. Buckingham), Cambridge University Press., Cambridge, **1994**; b) A. Lumbroso, M. L. Cooke, B. Breit, *Angew. Chem. Int. Ed.* **2013**, *52*, 1890–1893; *Angew. Chem.* **2013**, *125*, 1942–1986.

[17] The use of aliphatic alcohols has been much less studied than those using phenols. See: a) A. Iourtchenko, D. Sinou, *J. Mol. Catal. A* **1997**, *122*, 91–93; b) A. R. Haight, E. J. Stoner, M. J. Peterson, V. K. Grover, *J. Org. Chem.* **2003**, *68*, 8092–8096; c) F. L. Lam, T. T. L. Au-Yeung, F. Y. Kwong, Z. Zhou, K. Y. Wong, A. S. C. Chan, *Angew. Chem. Int. Ed.* **2008**, *47*, 1280–1283; *Angew. Chem.* **2008**, *120*, 1300–1303; d) F. Ye, Z.-J. Zheng, L. Li, K.-F. Yang, C.-G. Xia, L.-W. Xu, *Chem. Eur. J.* **2013**, *19*, 15452–15457; e) X. Caldentey, M. A. Pericàs, *J. Org. Chem.* **2010**, *75*, 2628–2644; f) Z. Liu, H. Du, *Org. Lett.* **2010**, *12*, 3054–3057; g) M. Kato, T. Nakamura, K. Ogata, S.-I. Fukuzawa, *Eur. J. Org. Chem.* **2009**, 5232–5238; h) B. Feng, H.-G. Cheng, J.-R. Chen, Q.-R. Deng, L. Q. Lu, W.-J. Xiao, *Chem. Commun.* **2014**, *50*, 9550–9553.

[18] a) J. D. Oslob, B. Äkermark, P. Helquist, P.-O. Norrby, *Organometallics* **1997**, *16*, 3015–3021; b) H. Hagelin, B. Äkermark, P.-O. Norrby, *Organometallics* **1999**, *18*, 2884–2895.

Research Article
doi.org/10.1002/ejic.202100988

[19] a) H. Hagelin, M. Svensson, B. Äkermark, P.-O. Norrby, *Organometallics* **1999**, *18*, 4574–4583; b) C. Moberg, U. Bremberg, K. Hallman, M. Svensson, P.-O. Norrby, A. Hallberg, M. Larhed, I. Csöregh, *Pure Appl. Chem.* **1999**, *71*, 1477–1483.

[20] In this study, only the two *syn-syn* allyl complexes were taken into account, neglecting the contribution of the *anti-anti* and *syn-anti* allylic species of higher energy.

[21] a) P. Fristrup, M. Ahlquist, D. Tanner, P.-O. Norrby, *J. Phys. Chem.* **2008**, *112*, 12862–12867; b) J. Wahlers, J. Margalef, E. Hansen, A. Bayesteh, P. Helquist, M. Diéguez, O. Pàmies, O. Wiest, P.-O. Norrby, *Nat. Commun.* **2021**, DOI: 10.1038/s41467-021-27065-2.

[22] a) P. R. Auburn, P. B. Mackenzie, B. Bosnich, *J. Am. Chem. Soc.* **1985**, *107*, 2033–2046; b) C. Jia, P. Müller, H. Mimoun, *J. Mol. Cat. A: Chem.* **1995**, *101*, 127–136; c) J. Lehman, G. C. Lloyd-Jones, *Tetrahedron* **1995**, *51*, 8863–8874; d) T. Hayashi, A. Yamamoto, Y. Ito, E. Nishioka, H. Miura, K. Yanagi, *J. Am. Chem. Soc.* **1989**, *111*, 6301–6311.

[23] M. J. Frisch, G. W. Trucks, H. B. Schlegel, G. E. Scuseria, M. A. Robb, J. R. Cheeseman, G. Scalmani, V. Barone, G. A. Petersson, H. Nakatsuji, X. Li, M. Caricato, A. V. Marenich, J. Bloino, B. G. Janesko, R. Gomperts, B. Mennucci, H. P. Hratchian, J. V. Ortiz, A. F. Izmaylov, J. L. Sonnenberg, D. Williams-Young, F. Ding, F. Lipparini, F. Egidi, J. Goings, B. Peng, A. Petrone, T. Henderson, D. Ranasinghe, V. G. Zakrzewski, J. Gao, N. Rega, G. Zheng, W. Liang, M. Hada, M. Ehara, K. Toyota, R. Fukuda, J. Hasegawa, M. Ishida, T. Nakajima, Y. Honda, O. Kitao, H. Nakai, T. Vreven, K. Throssell, J. A. Montgomery, J. E. Peralta, F. Ogliaro, M. J. Bearpark, J. J. Heyd, E. N. Brothers, K. N. Kudin, V. N. Staroverov, T. A. Keith, R. Kobayashi, J. Normand, K. Raghavachari, A. P. Rendell, J. C. Burant, S. S. Iyengar, J. Tomasi, M. Cossi, J. M. Millam, M. Klene, C. Adamo, R. Cammi, J. W. Ochterski, R. L. Martin, K. Morokuma, O. Farkas, J. B. Foresman, D. J. Fox, *Gaussian 16, Revision A.03*, Gaussian, Inc., Wallingford CT, **2016**.

[24] a) C. Lee, W. Yang, R. G. Parr, *Phys. Rev. B* **1988**, *37*, 785–789; b) A. D. Becke, *J. Chem. Phys.* **1993**, *98*, 5648–5652.

[25] P. J. Hay, W. R. Wadt, *J. Chem. Phys.* **1985**, *82*, 299–310.

[26] a) W. J. Hehre, R. Ditchfeld, J. A. Pople, *J. Chem. Phys.* **1972**, *56*, 2257–2261; b) P. C. Hariharan, J. A. Pople, *Theor. Chim. Acta* **1973**, *28*, 213–222; c) M. M. Francl, W. J. Pietro, W. J. Hehre, J. S. Binkley, M. S. Gordon, D. J. Defrees, J. A. Pople, *J. Chem. Phys.* **1982**, *77*, 3654–3665.

[27] a) S. Miertus, J. Tomasi, *Chem. Phys.* **1982**, *65*, 239–245; b) B. Mennucci, J. Tomasi, *J. Chem. Phys.* **1997**, *106*, 5151–5158; c) M. Cossi, V. Barone, B. Mennucci, J. Tomasi, *Chem. Phys. Lett.* **1998**, *286*, 253–260.

[28] a) R. Krishnan, J. S. Binkley, R. Seeger, J. A. Pople, *J. Chem. Phys.* **1980**, *72*, 650–654; b) A. D. McLean, G. S. Chandler, *J. Chem. Phys.* **1980**, *72*, 5639–5648.

[29] a) S. Grimme, J. Antony, S. Ehrlich, H. Krieg, *J. Chem. Phys.* **2010**, *132*, 154104–154119; b) S. Grimme, S. Ehrlich, L. Goerigk, *J. Comput. Chem.* **2011**, *32*, 1456–1465.

[30] a) E. Johnson, S. Keinan, P. Mori-Sánchez, J. Contreras-García, A. Cohen, W. Yang, *J. Am. Chem. Soc.* **2010**, *132*, 6498–6506; b) J. Contreras-García, E. Johnson, S. Keinan, R. Chaudret, J. Piquemal, D. Beratan, W. Yang, *J. Chem. Theory Comput.* **2011**, *7*, 625–632; c) J. Contreras-García, W. Yang, E. J. Johnson, *Phys. Chem. A* **2011**, *115*, 12983–12990.

Manuscript received: November 17, 2021
Revised manuscript received: January 18, 2022
Accepted manuscript online: January 19, 2022